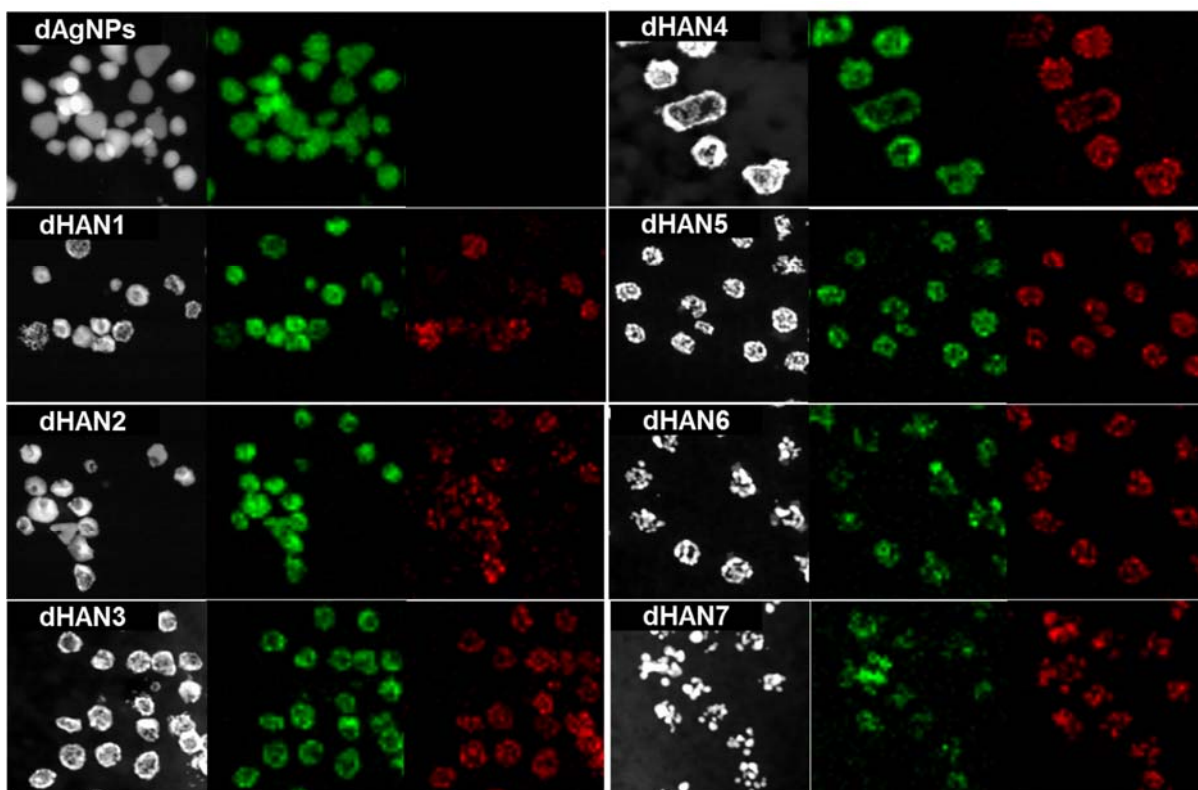


# Supporting Information

## Facile Synthesis and Intraparticle Self-catalytic Oxidation of Dextran-coated Hollow Au-Ag Nanoshell and Its Application for Chemo- Thermotherapy

*Hongje Jang, Young-Kwan Kim, Hyun Huh, Dal-Hee Min\**

Department of Chemistry, Seoul National University, Seoul, 151-747, Republic of Korea



**Figure S1.** HAADF-STEM | EDS analysis of dAgNPs and various dHANs against Ag and Au element. In elemental mapping images, green and red pixels represent Ag and Au element, respectively.

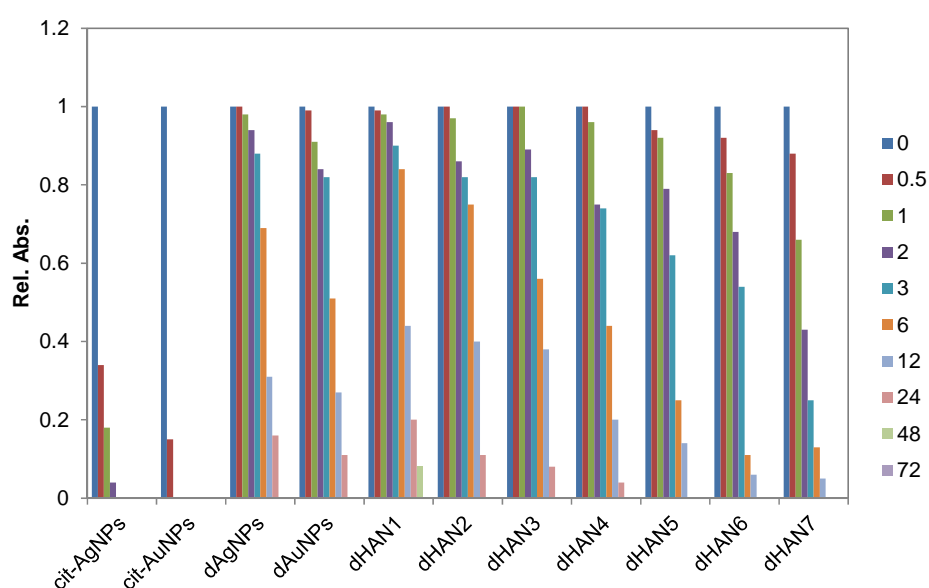


**Figure S2.** Colloidal stability test of various Au-Ag nanostructures at high temperature. Nanoparticles were incubated at 100°C using a thermo-cycler and UV-Vis absorbance was measured to estimate concentration of intact nanostructures at designated time points (0~72 hrs). Control nanoparticles (citrate stabilized AgNPs and AuNPs) showed poor colloidal stability at 100°C but the dextran coated nanoparticles and alloy shells showed relatively high stability under the same condition.

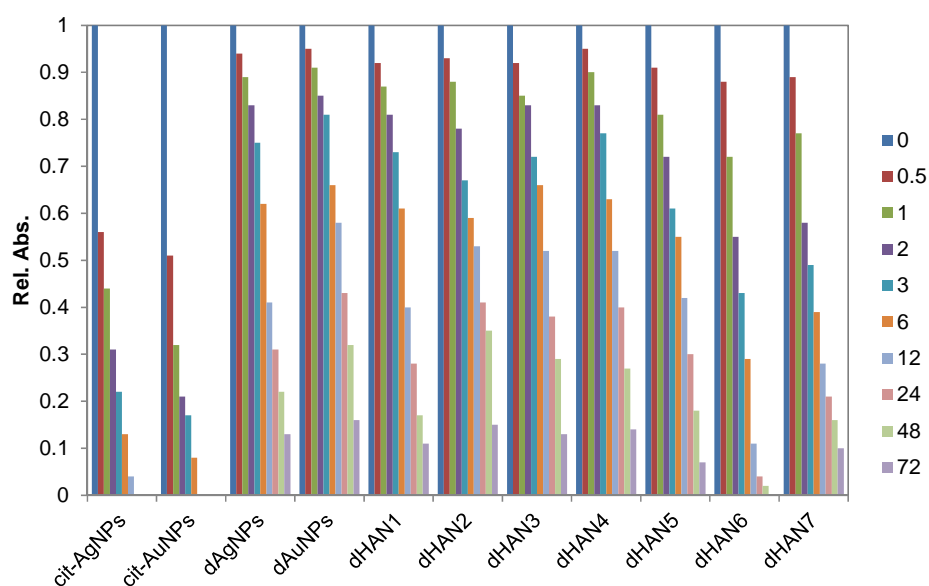


**Figure S3.** Colloidal stability test of various Au-Ag nanostructures at high salt concentration. Nanoparticles were incubated in 1 M NaCl solution and UV-Vis absorbance was measured to estimate concentration of intact nanostructures at designated time points (0~72 hrs). Control nanoparticles (citrate stabilized AgNPs and AuNPs) showed poor colloidal stability in 1 M NaCl solution but the dextran coated nanoparticles and alloy shells showed relatively high stability under the same condition.

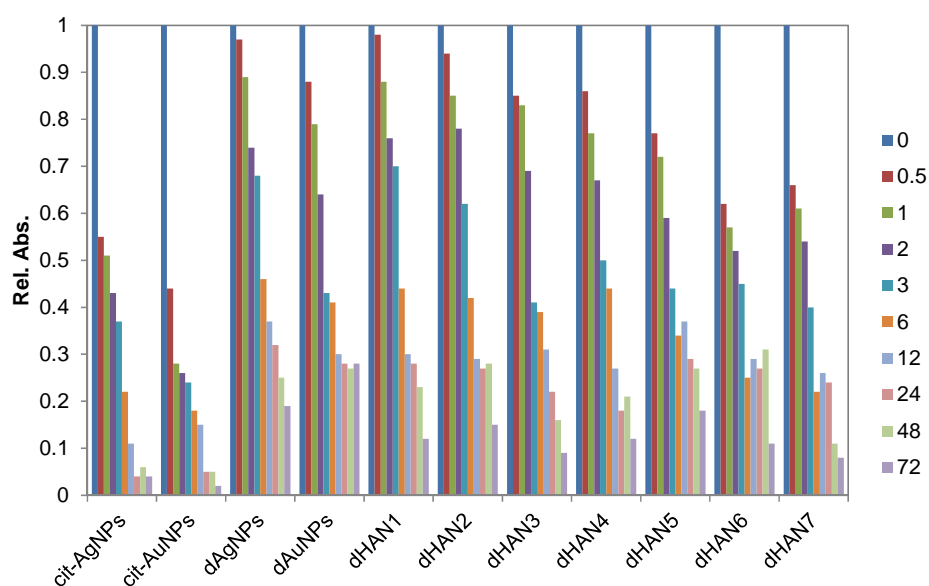


**Figure S4.** Colloidal stability test of various Au-Ag nanostructures at acidic pH. Nanoparticles were incubated in pH 2 solution (adjusted by using HCl) and UV-Vis absorbance was measured to estimate concentration of intact nanostructures at designated time points (0~72 hrs). Control nanoparticles (citrate stabilized AgNPs and AuNPs) showed poor colloidal stability at pH 2 but the dextran coated nanoparticles and alloy shells showed relatively high stability under the same condition.

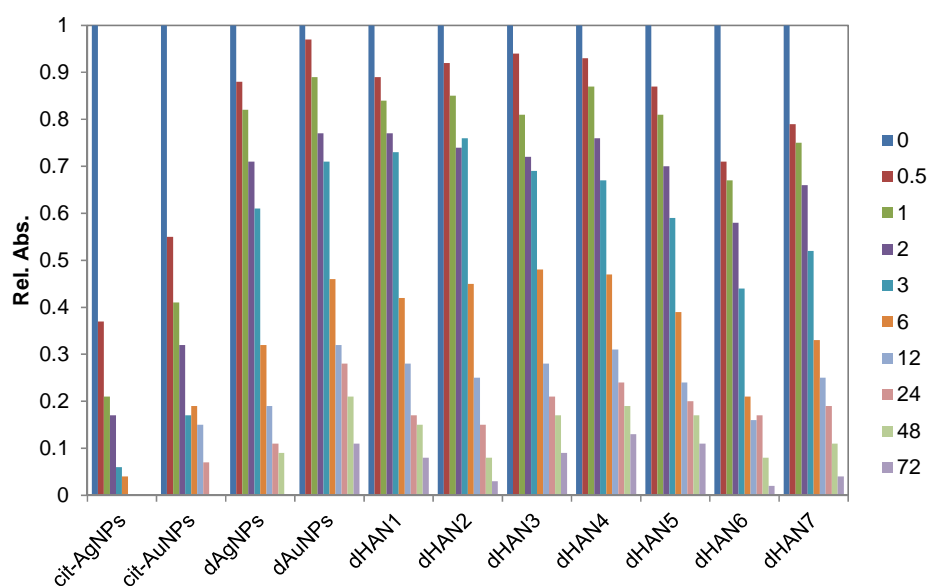


**Figure S5.** Colloidal stability test of various Au-Ag nanostructures at basic pH. Nanoparticles were incubated in pH 12 solution (adjusted by using NaOH) and UV-Vis absorbance was measured to estimate concentration of intact nanostructures at designated time points (0~72 hrs). Control nanoparticles (citrate stabilized AgNPs and AuNPs) showed poor colloidal stability at pH 12 but the dextran coated nanoparticles and alloy shells showed relatively high stability under the same condition.

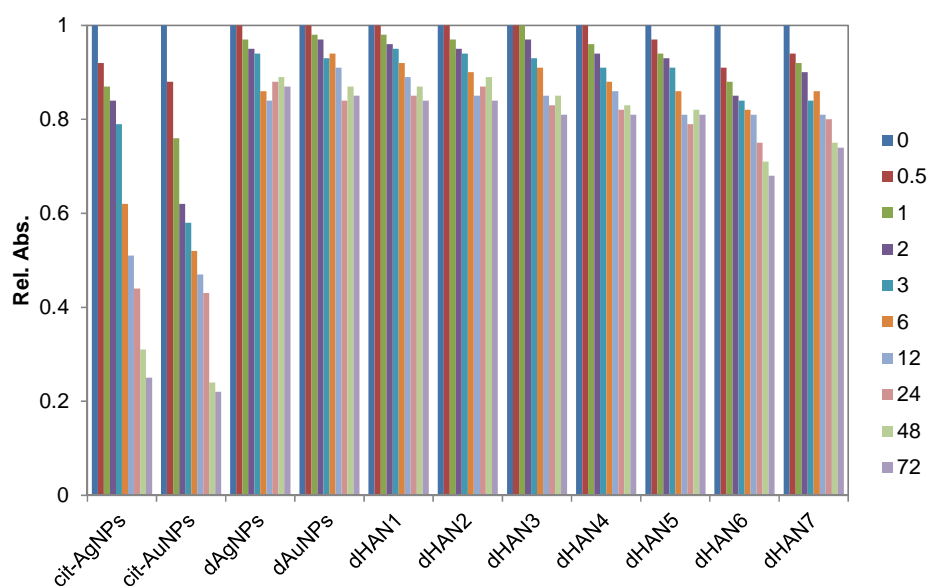


**Figure S6.** Colloidal stability test of various Au-Ag nanostructures in a biological buffer, 1X phosphate buffered saline (PBS). Nanoparticles were incubated in 1X PBS and UV-Vis absorbance was measured to estimate concentration of intact nanostructures at designated time points (0~72 hrs). Control nanoparticles (citrate stabilized AgNPs and AuNPs) showed poor colloidal stability in 1X PBS solution but the dextran coated nanoparticles and alloy shells showed very high stability under the same condition.

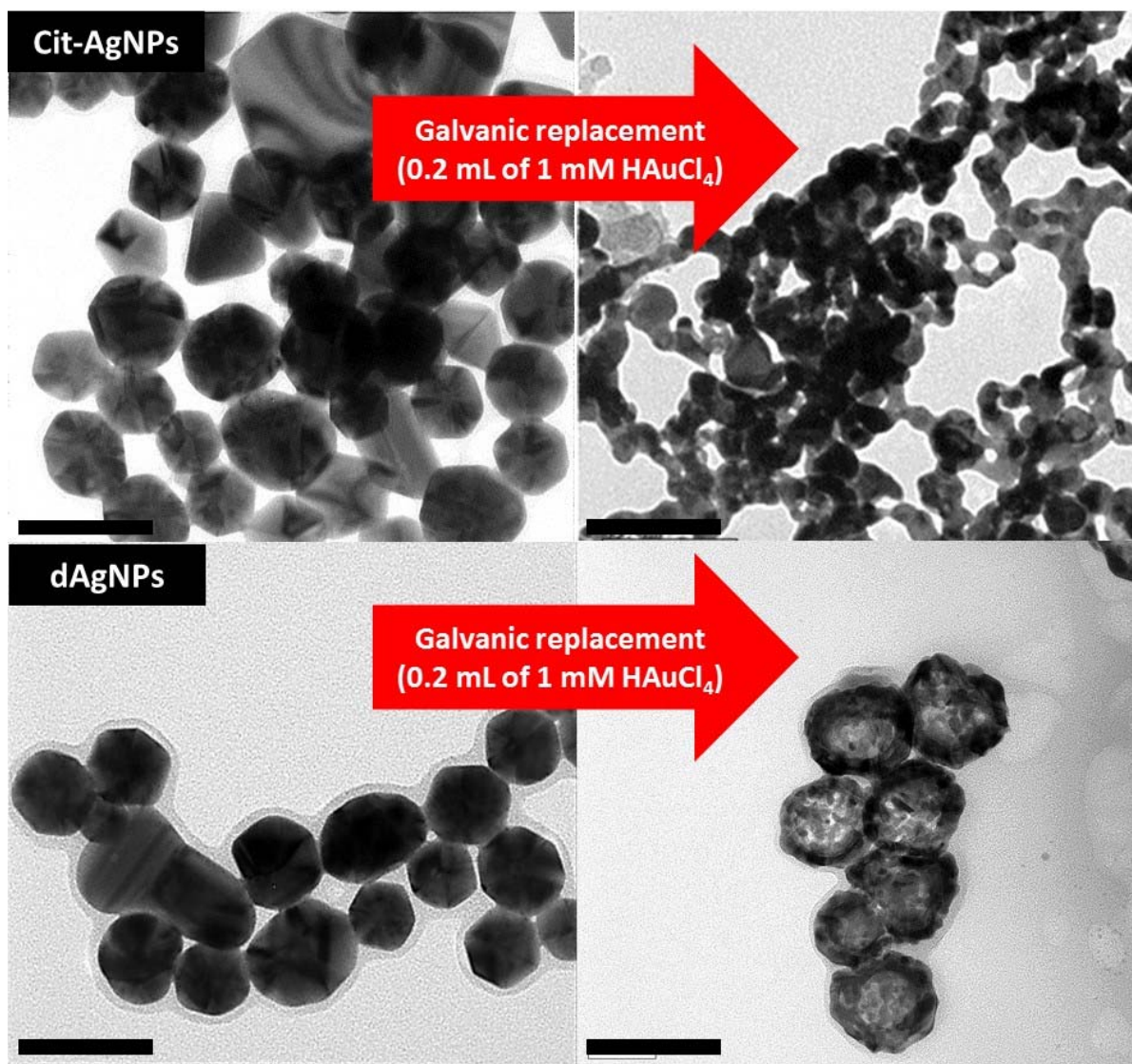


**Figure S7.** TEM images of cit-AgNPs, dAgNPs and their products obtained after galvanic replacement reaction with 0.2 mL of 1 mM HAuCl<sub>4</sub>. The presence of surface dextran coating prevented structural collapse during galvanic replacement reaction. The scale bar is 50 nm.

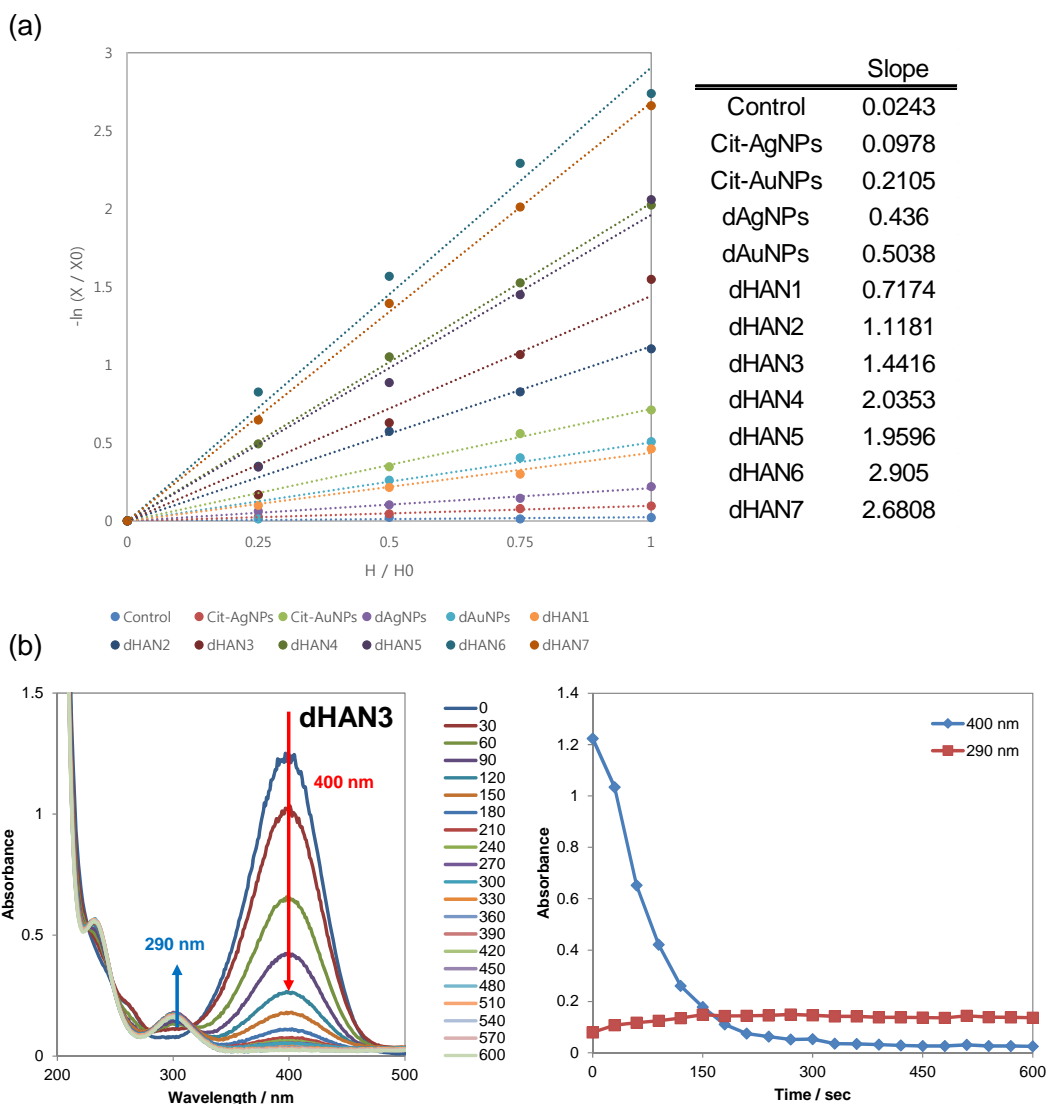


**Figure S8.** Catalytic activity measurement of Au-Ag nanostructures by using 4-nitrophenol reduction reaction. (a) Initial velocity of the catalytic reactions was estimated by calculating the slopes of the log form of relative decrease in absorbance peak corresponding to the substrate (4-nitrophenol) at 400 nm versus time interval from the addition of nanoparticles to 4-nitrophenolate in a quartz cuvette cell (H: incubation time, H<sub>0</sub>: total incubation time (120 sec)). (b) UV-Vis absorbance changes observed as the catalytic reaction went on for 600 sec with dHAN3 (left) and a graph plotted absorption intensity at 290 (4-aminophenol) and 400 nm (4-nitrophenolate ion) versus incubation time.

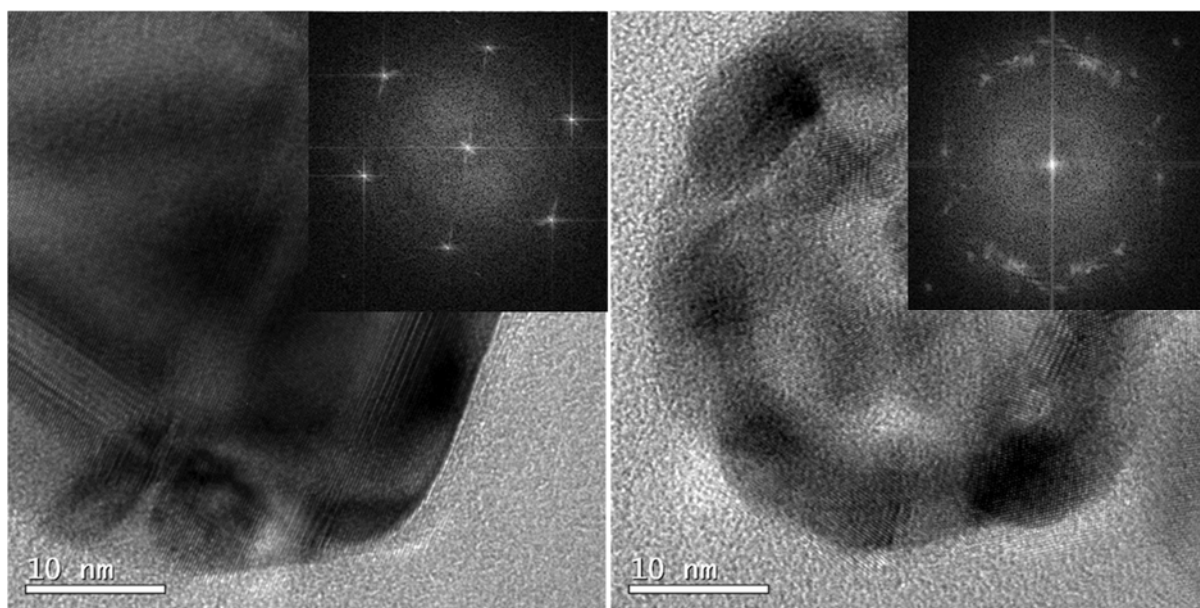


**Figure S9.** HR-TEM image and FFT analysis data. FFT explained catalytically active (111) facet orientation with multiple twins.

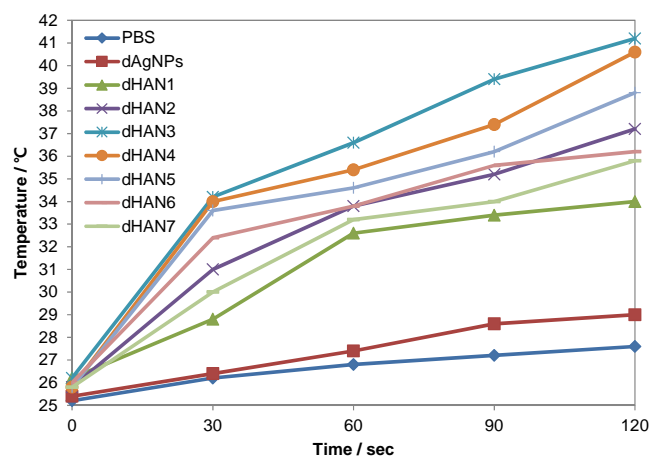


**Figure S10.** Temperature elevation of aqueous dHANs suspension (100 pM) under NIR laser irradiation (808 nm, 0.4 W/cm<sup>2</sup>) for 2 min was measured by using an IR thermogun. 1X PBS control set showed only 1.6°C increase but the NIR absorbing dHANs showed temperature increase up to 41.2°C within 120 sec.

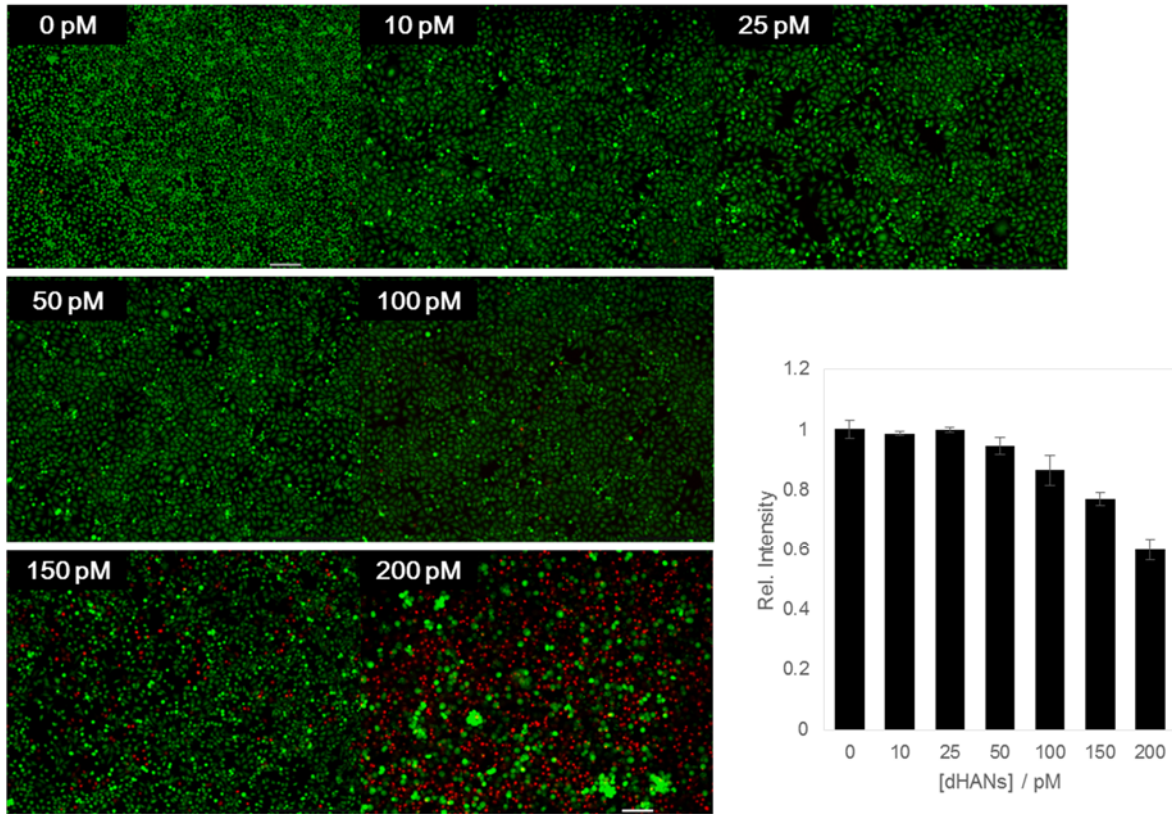


**Figure S11.** Cell viability test of dHAN3 against HeLa cell line. Cell viability was higher than 95% up to 50 pM of dHAN3 treatment and decreased down to 60% with 200 pM of dHAN3. Fluorescence images from Live/Dead staining was also shown.